Optical ridge waveguides in Nd:LGS crystal produced by combination of swift C5+ ion irradiation and precise diamond blade dicing

Cheng, Y.; Lv, J.; Akhmadaliev, S.; Zhou, S.; Chen, F.;

February 2016

Optics and Laser Technology 81(2016), 122-126

DOI: https://doi.org/10.1016/j.optlastec.2016.02.009

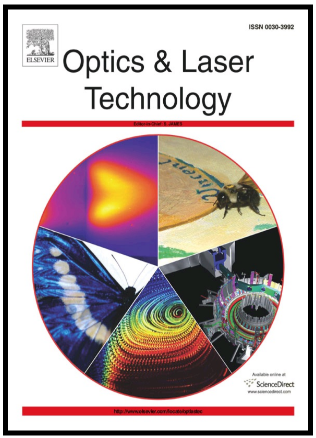

www.elsevier.com/locate/optlastec

Optical ridge waveguides in Nd:LGS crystal produced by combination of swift C^{5+} ion irradiation and precise diamond blade dicing

Yazhou Cheng, Jinman Lv, Shavkat Akhmadaliev,
Shengqiang Zhou, Feng Chen

PII: S0030-3992(15)30628-9
DOI: http://dx.doi.org/10.1016/j.optlastec.2016.02.009
Reference: JOLT3931

To appear in: *Optics and Laser Technology*

Received date: 17 November 2015
Revised date: 6 January 2016
Accepted date: 8 February 2016

Cite this article as: Yazhou Cheng, Jinman Lv, Shavkat Akhmadaliev, Shengqiang Zhou and Feng Chen, Optical ridge waveguides in Nd:LGS crysta produced by combination of swift C^{5+} ion irradiation and precise diamond blad dicing, *Optics and Laser Technolog* http://dx.doi.org/10.1016/j.optlastec.2016.02.009

Optical ridge waveguides in Nd:LGS crystal produced by combination of swift C^{5+} ion irradiation and precise diamond blade dicing

Yazhou Cheng[a], Jinman Lv[a], Shavkat Akhmadaliev[b], Shengqiang Zhou[b], Feng Chen[a,*]

[a]School of Physics, State Key Laboratory of Crystal Materials and Key Laboratory of Particle Physics and Particle Irradiation (MOE), Shandong University, Jinan 250100, China

[b]Helmholtz-Zentrum Dresden-Rossendorf, Institute of Ion Beam Physics and Materials Research, Dresden 01314, Germany

[*]Corresponding author. Tel.:+86 531 88363007; fax: +86 531 88363350. drfchen@sdu.edu.cn (F. Chen)

Abstract

We report on the fabrication of optical ridge waveguides in Nd:LGS crystal by using combination of swift C^{5+} ion irradiation and precise diamond blade dicing. The ridge structures support guidance both at 632.8 nm and 1064 nm wavelength along the TE and TM polarizations. The lowest propagation losses of the ridge waveguide for the TM mode are ~1.6 dB/cm at 632.8 nm and ~1.2 dB/cm at 1064 nm, respectively. The investigation of micro-fluorescence spectra and micro-Raman spectra indicates that the Nd^{3+} luminescence features have been well preserved and the microstructure of the waveguide region has no significant change after C^{5+} ion irradiation.

Keywords: Optical waveguide; Nd:LGS crystal; Ion irradiation; Diamond blade dicing

1. Introduction

As one of the most intriguing piezoelectric materials, lanthanum gallium silicate ($La_3Ga_5SiO_{14}$, or LGS) crystal has attracted considerable attention owing to its promising applications in surface acoustic wave (SAW) and bulk acoustic wave (BAW) technologies [1,2]. The LGS single crystal is usually grown via the conventional Czochralski technique [3] and belongs to the point group 32 and space group p321 [4]. It possesses the outstanding properties of relatively high electromechanical coupling coefficient [5,6], and therefore allows the development of new-generation miniature communication devices [7,8]. As the LGS crystal does not undergo any phase transitions and retains its piezoelectric properties until the melting temperature of 1470°C [9], it is particularly applied in high-temperature microbalances and gas sensors. In addition, when doped with Nd^{3+} ions, the Nd:LGS crystal can be used as an excellent gain medium for both continuous-wave (CW) and Q-switched laser generation systems [10]. With the broad emission bands and large birefringence, Nd:LGS crystal is also applicable for self-tunable laser gain operation using laser diode pumping [11].

Optical waveguides are basic components in integrated photonics, which can confine the light propagation in very small volumes with dimensions of several microns, achieving relatively higher optical intensities with respect to the bulk. Several techniques, such as metal-ion indiffusion [12], ion exchange [13], epitaxial layer deposition [14], ion implantation/irradiation [15,16], and femtosecond (fs) laser micromachining [17-20] have been used to fabricate optical waveguides in various materials. The swift heavy ion irradiation (usually with energy higher than 1 MeV) is an efficient technique to modify the refractive index of the materials for optical waveguide construction. Compared with normal ion implantation (with energy of 400 keV to a few MeV), swift heavy ion irradiation has advantages of ultralow ion fluences and reduced irradiation time for effective refractive index changes. In addition, during swift heavy ion irradiation process, the electronic damage created by the incident ions is dominant over the nuclear damage during most of the ion trajectory [21], which is different from the normal light ion implantation mechanism (nuclear damage dominant). Different from one-dimensional (1D) waveguides (planar or slab waveguides), two-dimensional (2D) waveguides (typically with channel or ridge geometries) can confine light propagation in two transverse dimensions and achieve much higher optical density. In practice, 2D waveguides has attracted much attention due to the superior guiding performance and therefore be applied to the construction of more complex integrated photonic devices. In recent years, diamond blade dicing technique is becoming an increasingly fascinating technique to construct high-quality ridge waveguides owing to the advantages of precise cutting and surface polishing. As of yet, by utilizing technique of diamond blade dicing, ridge waveguides have been successfully fabricated in $LiNbO_3$ [22], PPMgSLN [23], Nd:CNGG [24] and Nd:YAG [25] crystals.

In this work, we have fabricated ridge waveguides in Nd:LGS crystal by using combination of swift C^{5+} ion irradiation and precise diamond blade dicing. The guiding properties, micro-fluorescence spectra and micro-Raman spectra of the Nd:LGS waveguides have been investigated in detail.

2. Experiments in details

The *x*-cut Nd:LGS crystal (doped with 1 at.% Nd^{3+} ions) used in this work was cut with dimensions of 10 (*x*) × 10 (*y*) × 2 (*z*) mm^3 and was polished to high optical quality. Figure 1 depicts the schematic fabrication process of the Nd:LGS ridge waveguides. In the first step, one of the sample surface (10 (*x*) × 10 (*y*) mm^2) was irradiated with C^{5+} ions at energy of 17 MeV and fluence of 2×10^{14} ions/cm^2 by utilizing the 3 MV tandem accelerator at Helmholtz Zentrum Dresden-Rossendorf, Germany. The incident ions beam was tilted by 7° off the normal direction of the sample surface to minimize the channeling effect and the ion current density was kept at a low level (around 6-8 nA/cm^2) to avoid the heating and charging of the sample. In this way, a planar waveguide layer with a thickness of 10 μm was formed beneath the crystal surface. In the second step, we utilized a rotating diamond blade (with the rotating velocity of 10.000 rpm), which moved along the *x*-axis of the sample (with the moving speed of 0.1 mm/s), to construct parallel air grooves on the planar waveguide layer [26]. The width of the ridge structure was determined by modulating the separation of two adjacent air grooves. With the present parameters of the diamond blade dicing, the minimal width of the ridge waveguide is approximately ~13 μm for Nd:LGS crystal waveguide. Consequently two high-quality ridge waveguides WG1 (with width of 20 μm) and WG2 (with width of 40 μm) were constructed in Nd:LGS crystal. In order to improve the thermal stability and guiding properties, the sample was annealed at 200°C in air for 30 min.

A microscope (Axio Imager, Carl Zeiss) operating in transmission mode was employed to photograph the cross sections of the waveguides in Nd:LGS crystal. We applied a typical end-face coupling arrangement, as shown in Fig. 2, to investigate the guiding properties of the waveguides at 632.8 nm (He-Ne laser) and 1064 nm (Nd:YVO_4 solid-state laser), respectively. A pair of microscope objective lenses (25×) were used to couple the linearly polarized laser beam which was controlled by a polarizer into and out of the waveguides and finally the modal profiles were recorded by a CCD camera. We measured the input and output light power of the waveguides using the optical power meter, and calculated the transmittance ratio of the microscope objective lens and the transmittance ratio of the sample, and estimated the coupling efficiency between the input light and the guided mode of the waveguide, and thus obtained the propagation loss of the waveguide.

In order to study the physical mechanism of 17 MeV C^{5+} ion irradiated Nd:LGS ridge waveguide formation, we measured confocal micro-luminescence spectra and micro-Raman spectra of the sample by using the spectrometer (Horiba/Jobin Yvon HR800) at room temperature. A continuous wave laser at wavelength of 473 nm was focused onto the end facet of the sample (with the spot diameter of 1 μm) to detect the micro-luminescence and micro-Raman spectra of the waveguide and substrate region, respectively. The micro-luminescence spectra were recorded in the wavelength range of 840-940 nm and the micro-Raman spectra was carried out in the frequency range of 140 cm^{-1}-820 cm^{-1} with a wavenumber precision of 2 cm^{-1}.

3. Results and discussion

To investigate the mechanism of the refractive-index modification of the ion irradiated region of the sample, we simulated the energy deposition process of the 17 MeV C^{5+} ion irradiation on Nd:LGS crystal using the software Stopping and Range of Ions in Matter (SRIM-2011) code [27]. Figure 3(a) depicts the electronic and nuclear stopping powers (S_e and S_n) of the 17 MeV C^{5+} ions as the function of penetration depth inside the Nd:LGS crystal. As we can see, S_e is dominant over S_n in the first 0-9 µm, peaking at 2.1 keV/nm at a depth of ~6.8 µm. In the meantime, S_n remains nearly zero in the first 0-8 µm and climbs to a peak value of 0.17 keV/nm at a depth of ~9.5 µm. It suggests that in this case, the electronic damage is dominant over the nuclear damage during most of the ion trajectory and the electronic damage is the critical factor for the waveguide refractive-index modification.

Assuming a step-index profile and measuring the N.A. of the waveguide, we can estimate the maximum refractive index contrast of the waveguide through the formula [28]

$$\Delta n = \frac{\sin^2 \Theta_m}{2n} \tag{1}$$

where n is the refractive index of the substrate material at 1064 nm, Θ_m is the maximum incident angular deflection at which no change of the transmitted power is occurring. The resulting value of the maximum refractive index contrast of the waveguide was estimated $\Delta n_\mathrm{TE} \approx +0.004$ for TE polarization and $\Delta n_\mathrm{TM} \approx +0.006$ for TM polarization at 1064 nm. An error of 30% was estimated due to uncertainty of the measured maximum incident angular deflection [28]. Combining the maximum refractive index contrast value with the electronic stopping power profile, we could reconstruct the refractive index change distribution of the waveguide at 1064 nm for both TE and TM polarization (see Fig. 3(b)). As we can see, the maximum refractive index contrast of the waveguide for TM polarization is larger than that for TE polarization, which indicates that the Nd:LGS ridge waveguide could confine the light propagation on TM mode more efficiently than that on TE mode at 1064 nm.

Figures 4(a), 4(d) and 4(g) show the microscope images of the cross section of the planar and ridge waveguides (WG1 and WG2) in Nd:LGS crystal, respectively. As we can see, the ion beam modified region has a thickness of ~10 μm, which is in good agreement with the projected range of the 17 MeV C^{5+} ions in Nd:LGS crystal calculated by SRIM-2011 code. Figures 4(b), 4(e) and 4(h) depict the measured near-field modal profiles of the planar and ridge waveguides (WG1 and WG2) in Nd:LGS crystal at 632.8 nm along TM polarization, respectively. Figures 4(c), 4(f) and 4(i) show the measured near-field modal profiles of the planar and ridge waveguides (WG1 and WG2) in Nd:LGS crystal at 1064 nm along TM polarization, respectively. We can find that, for the planar waveguide, TM_0 modes are formed both at 632.8 nm and 1064 nm. The ridge waveguide WG1 supports light guidance (TM_{00}) both at 632.8 nm and 1064 nm. For the ridge waveguide WG2, a TM_{20} mode is observed at 632.8 nm and a TM_{00} mode is observed at 1064 nm. Based on the reconstructed refractive index change profile, we simulated 2D modal profiles of the planar and ridge waveguide WG1 at 1064 nm for TM polarization by using the software Rsoft© Beam-Prop [29] through Finite-Difference Beam Propagation Method (FD-BPM) [30], as shown in Figs. 5(a) and 5(b). As we can see, the simulated modal profiles of the planar and ridge waveguide WG1 are in good agreement with the experimental results, which indicates that the reconstructed refractive index change profile of the waveguide at 1064 nm is reasonable.

Table 1. Propagation losses of the planar and ridge waveguides (WG1 and WG2) at 632.8 nm and 1064 nm

waveguides	Propagation loss (dB/cm)			
	632.8 nm		1064 nm	
	TE	TM	TE	TM
planar	1.1	0.8	0.9	0.7

WG1	2.1	1.7	1.7	1.4
WG2	1.8 (TE_{20})	1.6 (TM_{20})	1.5	1.2

Table 1 shows the propagation losses of the 17 MeV C^{5+} ion irradiated Nd:LGS planar and ridge waveguides (WG1 and WG2) for both TE and TM polarization, exhibiting in all the cases better performance for TM polarization. This effect was observed previously for the ridge waveguides in Nd:SLG and Nd:SGG produced by the similar techniques [31]. Compared to the Nd:SLG and Nd:SGG, the propagation losses in Nd:LGS ridge waveguides are somehow higher. Further optimization of the parameters of the dicing and irradiation may enable reduction of the propagation losses the Nd:LGS ridge waveguides. We can also find that as the width of the ridge waveguide structure increases, the propagation loss becomes lower. The propagation losses of the ridge waveguides are higher than the planar waveguide and the reason may be partly attributed to the roughness of the side-walls fabricated by the diamond ablation. For the same waveguide, the propagation loss at 1064 nm is lower than that at 632.8 nm, which indicates that 1064 nm is a prior transmission wavelength for the 17 MeV C^{5+} ion irradiated Nd:LGS waveguide.

The confocal micrometric techniques (photoluminescence, Raman, etc.) have been successfully applied to investigate the ion irradiated waveguides [32,33]. Figure

6 shows the confocal micro-fluorescence spectra corresponding to the $^4F_{3/2}\rightarrow{}^4I_{9/2}$ transition of Nd^{3+} ions obtained in the ridge waveguide and the bulk of Nd:LGS crystal at room-temperature. Comparing the spectra of the waveguide and the bulk, we can see that the peak widths, peak positions and spectra shape are basically resembled and only the spectra intensity of the waveguide has a slight increase compared to the bulk. It implies that swift C^{5+} ion irradiation does not induce any fluorescence quenching and the original photoluminescence features have been well preserved in the waveguide region, which shows potential applications for further waveguide laser operations.

Figure 7 depicts the confocal micro-Raman spectra in the ridge waveguide region and the bulk of Nd:LGS crystal at room-temperature. As we can see, the spectra of the ridge waveguide and the bulk have similar shape, peak widths and peak positions, while the peak intensities of the waveguide averagely decrease about 3% compared to the bulk. It indicates that as the little lattice modification induced by the low-fluence C^{5+} ion irradiation is far below the lattice damage threshold of Nd:LGS crystal, the C^{5+} ion irradiation does not modify the Nd:LGS crystal lattice significantly.

4. Conclusion

We have fabricated ridge waveguides in Nd:LGS crystal by using combination of swift C^{5+} ion irradiation and precise diamond blade dicing. The guiding properties of the waveguides both at 632.8 nm and 1064 nm have been investigated. Based on the reconstructed refractive index change profile, the calculated near-field modal profiles of the waveguides are in good agreement with the experimental results. The minimum propagation losses of the ridge waveguide for the TM mode are measured to be ~1.6 dB/cm at 632.8 nm and ~1.2 dB/cm at 1064 nm, respectively. The micro-fluorescence spectra demonstrate that the Nd^{3+} luminescence features have been well preserved in the C^{5+} ion irradiated waveguide region and the micro-Raman spectra indicate that there is no significant microstructural change in Nd:LGS crystal after swift C^{5+} ion irradiation.

Acknowledgements

The work is supported by the National Natural Science Foundation of China (No. U1332121). S.Z. acknowledges the funding by the Helmholtz-Gemeinschaft Deutscher Forschungszentren (HGF-VH-NG-713).

References

[1] H. Fritze, H.L. Tuller, Appl. Phys. Lett. 78 (2001) 976.

[2] S. Zhang, Y. Zheng, H. Kong, J. Xin, E. Frantz, J. Appl. Phys. 105 (2009) 114107.

[3] J. Bohm, R.B. Heimann, M. Hengst, R. Roewer, J. Schindler, J. Cryst. Growth 204 (1999) 128.

[4] A.A. Kaminskii, B.V. Mill, G.G. Khodzhabagyan, A.F. Konstantinova, A.I. Okorochkov, I.M. Silvestrova, Phys. Status Solidi A 80 (1983) 387.

[5] M. Kadota, J. Nakanishi, T. Kitamura, M. Kumatoriya, Jpn. J. Appl. Phys. 38 (1999) 3288.

[6] S. Uda, A. Bungo, C. Jian, Jpn. J. Appl. Phys. 38 (1999) 5516.

[7] M.P. Cunda, S.A. Fagundes, IEEE Trans. Sonics Ultrason. 46 (1999) 1583.

[8] M. Adachi, T. Karaki, W. Miyamoto, Jpn. J. Appl. Phys. 38 (1999) 3283.

[9] K. Shimamura, H. Takeda, T. Kohno, T. Fukuda, J. Cryst. Growth 163 (1996) 388.

[10] Y. Yu, J. Wang, H. Zhang, Z. Wang, H. Yu, M. Jiang, Opt. Lett. 34 (2009) 467.

[11] I. Aramburu, I. Iparraguirre, M. A. Illarramendi, J. Azkargorta, J. Fernandez, R. Balda, Opt. Mater. 27 (2005) 1692.

[12] M. Quintanilla, E.M. Rodríguez, E. Cantelar, F. Cussó, C. Domingo, Opt. Express 18 (2010) 5449.

[13] A. Tervonen, B.R. West, S. Honkanen, Opt. Eng. 50 (2011) 071107.

[14] R.W. Eason, T.C. May-Smith, C. Grivas, M.S.B. Darby, D.P. Shepherd, R. Gazia, Appl. Surf. Sci. 255 (2009) 5199.

[15] F. Chen, Laser Photon. Rev. 6 (2012) 622.

[16] Y. Tan, Q. Luan, F. Liu, S. Akhmadaliev, S. Zhou, F. Chen, Opt. Express 21 (2013) 13992.

[17] Y. Tan, Y. Yao, J.R. Macdonald, A.K. Kar, H. Yu, H. Zhang, F. Chen, Opt. Lett. 39 (2014) 5289.

[18] F. Chen, J.R. Vazquez de Aldana, Laser Photon. Rev. 8 (2014) 251.

[19] D. Choudhury, J.R. Macdonald, A.K. Kar, Laser Photon. Rev. 8 (2014) 827.

[20] T. Calmano, S. Müller, IEEE J. Sel. Top. Quantum Electron. 21 (2015) 1602213.

[21] J. Olivares, A. Garcia-Navarro, A. Mendez, F. Agullo Lopez, G. Garcia, A. Garcia-Cabanes, M. Carrascosa, Nucl. Instrum. Methods Phys. Res. B 257 (2007) 765.

[22] T. Nishikawa, A. Ozawa, Y. Nishida, M. Asobe, F.L. Hong, T.W. Hänsch, Opt. Express 17 (2009) 17792.

[23] T. Kishimoto, K. Nakamura, IEEE Photon. Technol. Lett. 23 (2011) 161.

[24] Q. Luan, Y. Tan, S. Akhmadaliev, S. Zhou, H. Yu, H. Zhang, F. Chen. Opt. Mater. 39 (2015) 247.

[25] Y. Jia, Ch. E. Rüter, Sh. Akhmadaliev, Sh. Zhou, Feng Chen, D. Kip, Opt. Mater. Express 3 (2013) 433-438.

[26] DISCO Corp., http://www.disco.co.jp/.

[27] J.F. Ziegler, computer code, SRIM http://www.srim.org.

[28] J. Siebenmorgen, T. Calmano, K. Petermann, G. Huber, Opt. Express 18 (2010) 16035.

[29] Rsoft Design Group, Computer Software BeamPROP version 8.0, http://www.rsoftdesign.com.

[30] D. Yevick, W. Bardyszewski, Opt. Lett. 17 (1992) 329.

[31] C. Chen, Q. Luan, R. He, C. Cheng, S. Akhmadaliev, S. Zhou, H. Yu, H. Zhang, F. Chen, Opt. Laser Technol. 68 (2015) 84.

[32] D. Jaque, F. Chen, Appl. Phys. Lett. 94 (2009) 011109.

[33] D. Jaque, F. Chen, Y. Tan, Appl. Phys. Lett. 92 (2008) 161908.

Figure Captions

Fig. 1. Schematic fabrication process of the Nd:LGS ridge waveguides: (a) 17 MeV C^{5+} ion irradiation and (b) diamond blade dicing.

Fig. 2. Schematic plot of the end-face coupling arrangement utilized to investigate the guiding properties of the Nd:LGS waveguides.

Fig. 3. (a) Electronic (blue line) and nuclear (red line) stopping powers as function of penetrate depth from the surface of the 17 MeV C^{5+} ion irradiated Nd:LGS crystal and (b) reconstructed refractive index change profile of the 17 MeV C^{5+} ion irradiated planar waveguide at 1064 nm for both TE (blue line) and TM (red line) polarization.

Fig. 4. Microscope images of the cross section (left) and measured near-field intensity distributions at 632.8 nm (middle) and 1064 nm (right) of the planar waveguide, ridge waveguide WG1 and ridge waveguide WG2 along TM polarization. (The dashed circle represents the position of the waveguide structure)

Fig. 5. Calculated modal profiles of the (a) planar waveguide and (b) ridge waveguide WG1 for TM polarization at 1064 nm by using FD-BPM code.

Fig. 6. Confocal micro-fluorescence spectra related to the $^4F_{3/2} \rightarrow {}^4I_{9/2}$ transition of Nd^{3+} ions obtained from the ridge waveguide (red dashed line) and the bulk (blue line) of the Nd:LGS crystal.

Fig. 7. Confocal micro-Raman spectra obtained from the ridge waveguide (red line) and the bulk (blue line) of the Nd:LGS crystal.

Highlights

- Ridge waveguides first fabricated in Nd:LGS crystal.
- Good guiding properties of ridge waveguides at 632.8 nm and 1064 nm.
- Fluorescence properties well preserved in waveguides.

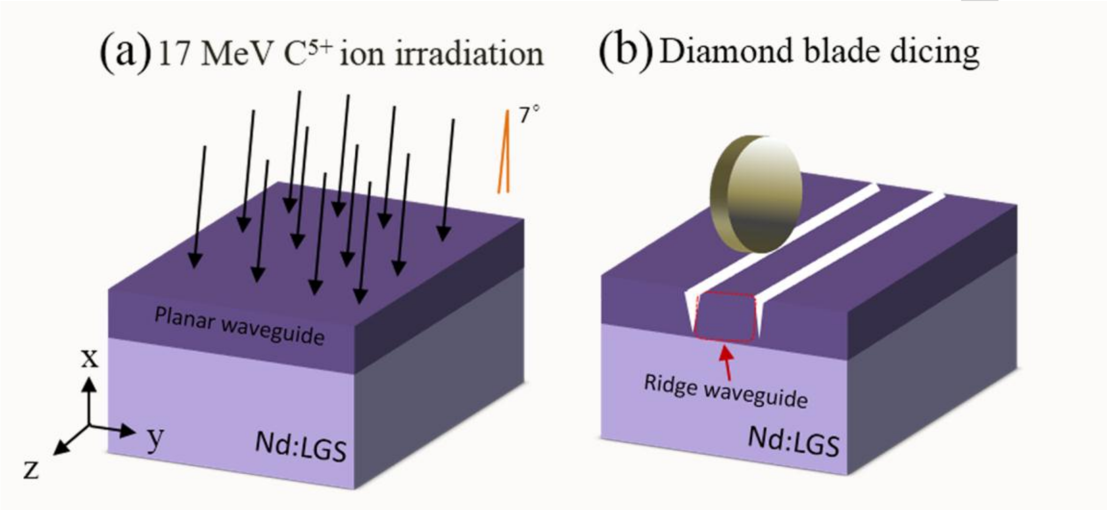

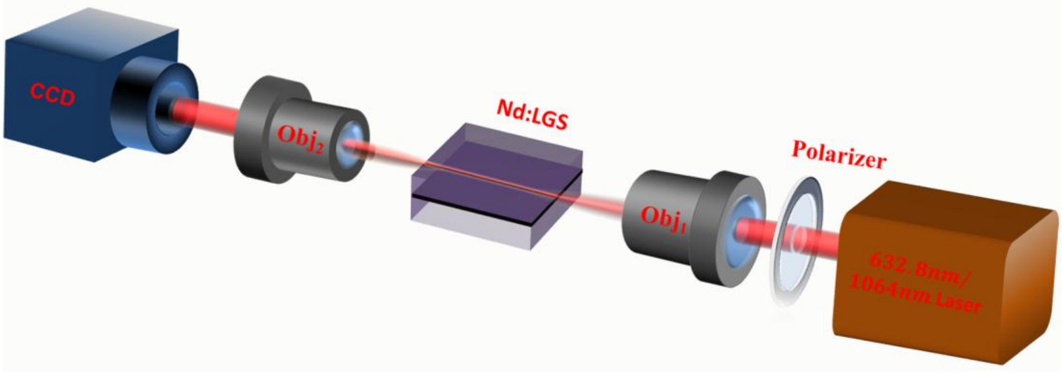

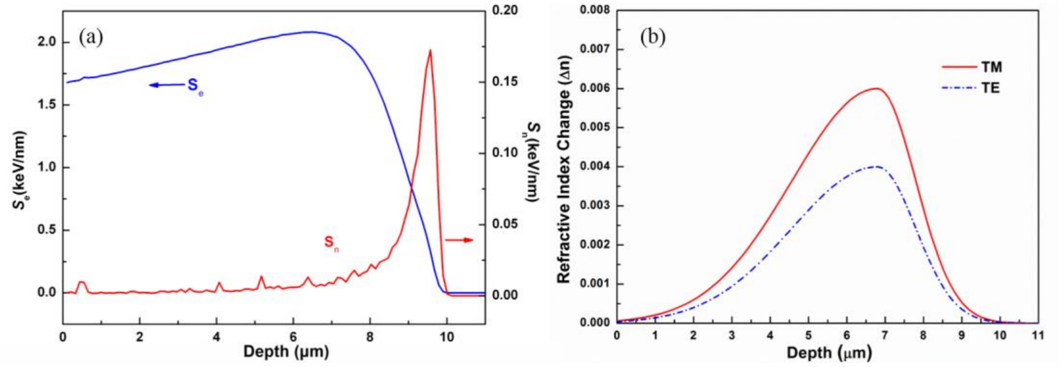
(a)
S_e
S_n
S_e(keV/nm)
S_n(keV/nm)
Depth (µm)
0.0
0.5
1.0
1.5
2.0
0.00
0.05
0.10
0.15
0.20
0
2
4
6
8
10
(b)
TM
TE
Refractive Index Change (Δn)
Depth (µm)
0.000
0.001
0.002
0.003
0.004
0.005
0.006
0.007
0.008
0
1
2
3
4
5
6
7
8
9
10
11

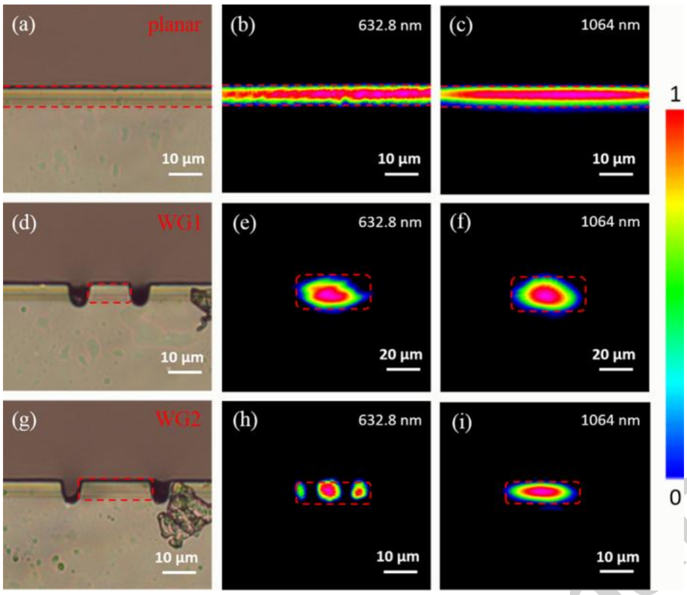
(a)
planar
10 µm
(b)
632.8 nm
10 µm
(c)
1064 nm
10 µm
(d)
WG1
10 µm
(e)
632.8 nm
20 µm
(f)
1064 nm
20 µm
(g)
WG2
10 µm
(h)
632.8 nm
10 µm
(i)
1064 nm
10 µm
1
0

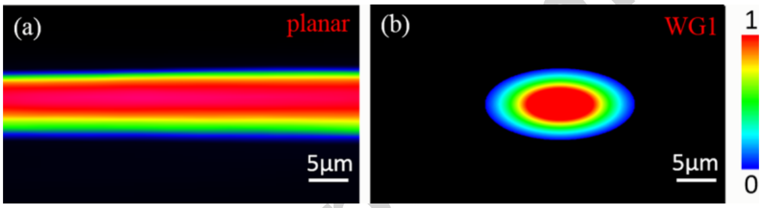
(a)
planar
5µm
(b)
WG1
5µm
1
0

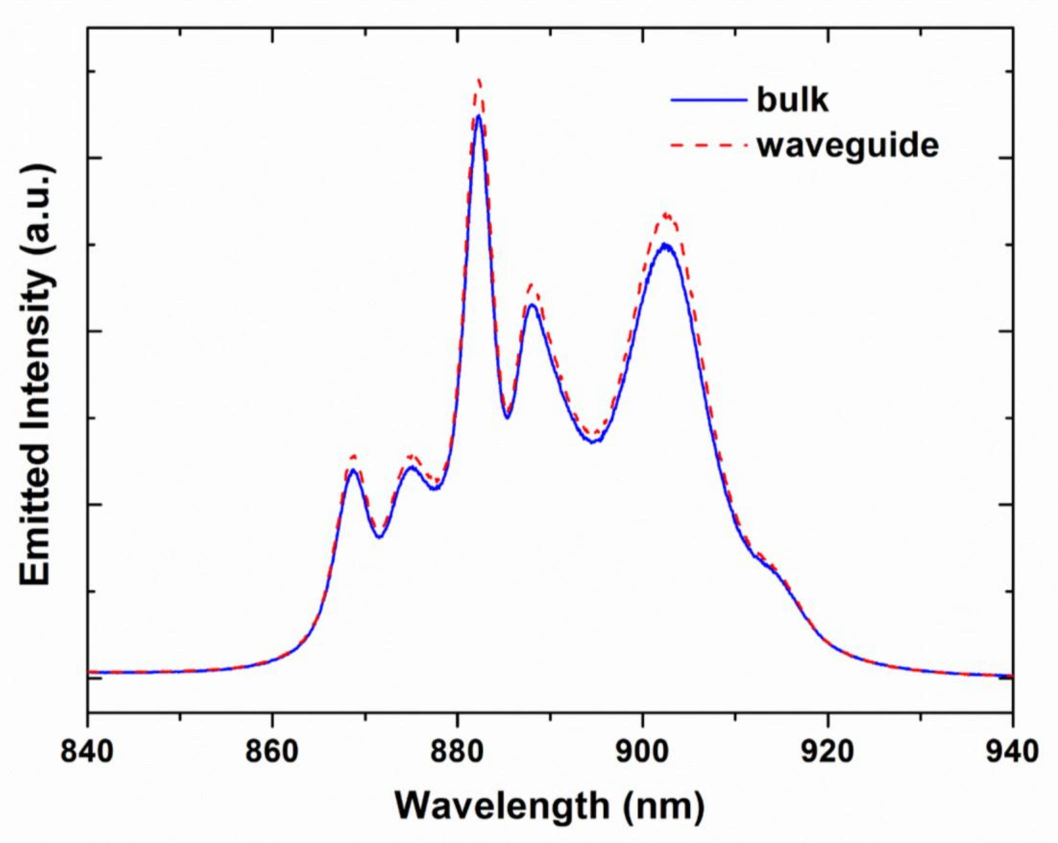
bulk
waveguide
Emitted Intensity (a.u.)
840
860
880
900
920
940
Wavelength (nm)

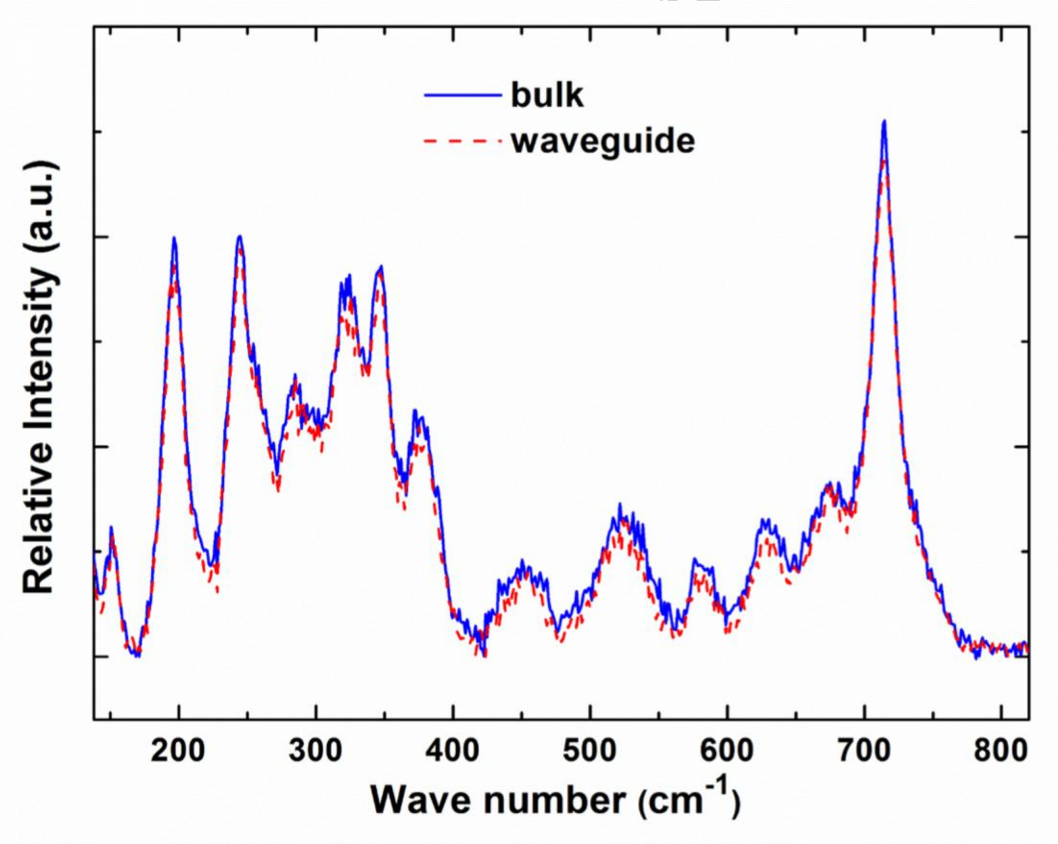
bulk
waveguide
Relative Intensity (a.u.)
200
300
400
500
600
700
800
Wave number (cm-1)